A novel pendrin inhibitor identified in a small molecule screen attenuates lipopolysaccharide-induced acute lung injury

Eun Hye Lee

Department of Medicine

The Graduate School, Yonsei University

A novel pendrin inhibitor identified in a small molecule screen attenuates lipopolysaccharide-induced acute lung injury

Directed by Professor Moo Suk Park

The Doctoral Dissertation
Submitted to the Department of Medicine,
the Graduate School of Yonsei University
in partial fulfillment of the requirements for the degree of
Doctor of Philosophy

Eun Hye Lee

June 2019

This certifies that the Doctoral Dissertation of Eun Hye Lee is approved.

Thesis Supervisor: Moo Suk Park

Thesis Committee Member #1: Young Sam Kim

Thesis Committee Member #2: Jae Young Choi

Thesis Committee Member #3: Jong Wook Shin

Thesis Committee Member #4: Hyo Sup Shim

The Graduate School
Yonsei University

June 2019

ACKNOWLEDGEMENTS

I would like to express my sincere gratitude to several people who supported me during the time of writing this doctoral dissertation.

First of all, I am deeply indebted to my supervisor Prof. Moo Suk Park for his patient guidance throughout the research work. Without his advice and unconditional support, I could not have completed this dissertation.

I am also very grateful to the members of my thesis committee, Prof. Young Sam Kim, Prof. Jae Young Choi, Prof. Jong Wook Shin, and Prof. Hyo Sup Shim. Thank you for your time and valuable comments on the thesis. I also thank Mi Hwa Shin, who has helped me a lot during the experiment. I would like to express my heartfelt gratitude to Prof. Young Ae Kang, who always gave me encouragements, support, and good advice.

I owe a lot to my parents and my sister, who helped me at every stage of my personal and academic life. Without their love and sacrifices, I could not have finished this dissertation. I would also like to thank my mother-in-law, my father-in-law, who encouraged and supported my studies.

I would like to dedicate this dissertation to my husband San Lee and my son Hyun Lee, and my lovely daughter Ann Lee, to whom my expression of love and gratitude is never enough.

Finally, I thank God for giving me infinite love and grace in my life.

TABLE OF CONTENTS

LIST OF FIGURES

LIST OF TABLES

ABSTRACT

A novel pendrin inhibitor identified in a small molecule screen attenuates lipopolysaccharide-induced acute lung injury

Eun Hye Lee

Department of Medicine
The Graduate School, Yonsei University

(Directed by Professor Moo Suk Park)

Purpose: Pendrin encoded by the SLC26A4 is an anion exchanger, and recent studies have shown that pendrin is up-regulated in airway disease such as chronic obstructive pulmonary disease (COPD), allergic rhinitis, asthma. However, studies on the role of pendrin in infection induced-acute lung injury (ALI) are lacking. We sought to identify the role of the pendrin and a novel pendrin inhibitor (YS-01) in lipopolysaccharide (LPS)-induced ALI mouse model

Methods: Wild-type mice were intranasally instilled LPS (10 μg/g) with DMSO or pendrin inhibitor (YS-01). Lung injury parameters were assessed in lung tissue and bronchoalveolar lavage fluid (BALF) and inflammatory cytokines were measured in lung lysates. For in vivo optical imaging (IVIS), transgenic NF-κB reporter/SPC-Cre-

ER^{T2} mice were used. Pendrin levels in BALF of 48 pneumonia patients and 25 patients with the non-infectious disease were also measured by ELISA.

Results: Compared to LPS with DMSO, LPS with YS-01 treated mice had attenuated lung injury and reduced cell counts and protein concentration of BALF. Proinflammatory cytokines were increased after LPS and suppressed after YS-01 treatment. NF-κB activation, analyzed by western blot and IVIS, was inhibited by YS-01 treatment in LPS-induced ALI mice. Furthermore, expressions of pendrin were also upregulated in BALF of pneumonia patients compared to BALF of patients with the non-infectious disease (mean, 22.65 vs. 6.83 ng/ml, $p<0.001$).

Conclusions: These results suggest that pendrin inhibitors could provide a novel strategy for the treatment of inflammatory airway diseases including sepsis-induced acute lung injury.

Keywords: pendrin, inhibitor, SLC26A4, acute lung injury

A novel pendrin inhibitor identified in a small molecule screen attenuates lipopolysaccharide-induced acute lung injury

Eun Hye Lee

Department of Medicine
The Graduate School, Yonsei University

(Directed by Professor Moo Suk Park)

I. INTRODUCTION

Acute lung injury (ALI), a common and severe pulmonary complication of critical illness, affects approximately 10 to 15% of patients hospitalized in the intensive care unit (ICU)[1]. Acute respiratory distress syndrome (ARDS), the most severe form of ALI, has a mortality rate of approximately 40%, despite modern ICU care[2,3]. Despite decades of research, treatment options for ARDS are limited and supportive care with mechanical ventilation remains the mainstay of management[4]. ARDS/ALI are characterized by the abrupt onset of hypoxemia with diffuse pulmonary infiltrates, it also an accumulation of a protein-rich pulmonary edema that causes reduction in lung compliance, alveolar collapse, and ventilation-perfusion mismatch[5]. Recent reports suggest that ion pump and channel functions are affected early during sepsis-induced ARDS[6], and airway epithelial cells may be a valuable therapeutic target for the treatment of ALI/ARDS.

Pendrin encoded by the *SLC26A4* acts as an anion exchanger which secrete Cl^- in

exchange with base such as HCO_3^-, I^-, OH^-, SCN^- and formate[7-10]. Pendrin is expressed in inner ear and thyroid and its mutation is associated with prelingual deafness (DFNB4) or Pendred syndrome[11,12]. Normal airway epithelium shows negligible pendrin expression. However, the expression of pendrin is strongly up-regulated in inflammatory airway diseases such as chronic obstructive pulmonary disease (COPD), allergic rhinitis, asthma[13,14]. The upregulation of pendrin is also observed in primary airway epithelial cells when they are cultured with IL-4, IL-13 and IL-17A[9,13,15]. Interestingly, the pendrin null mice showed reduced lung inflammation in response to Bordetella pertussis[16] and the prevalence of asthma among individuals with mutant pendrin is lower[13]. These evidences indicate that pendrin is one of critical protein in the pathogenesis of inflammatory airway disease. Recently, Dr. Verkman and his colleagues screened small-molecule for pendrin inhibitors and showed that several hit compounds for pendrin inhibitor significantly increased the thickness of airway surface liquid in cystic fibrosis patient's bronchial epithelial cells expressing high levels of pendrin[17]. We also performed a cell-based high throughput screening for the identification of small-molecule pendrin inhibitors. The pendrin inhibitor we screened (YS-01) showed a strongly therapeutic effect in OVA-induced allergy asthma murine model, where it inhibited pendrin/$OSCN^-$/NF-κB-mediated airway inflammation.

Recent data showed that pendrin is also expressed in alveolar epithelia and administration of non-specific anion exchanger inhibitor (methazolamide) attenuates LPS-induced ALI phenotype[18]. Our preliminary data showed that the levels of pendrin expression was up-regulated in bronchoalveolar lavage fluid samples from patients with pneumonia/ARDS Although, the pathophysiological roles of pendrin in ALI are not clearly understood, these emerging evidence indicates that pendrin can be a novel drug target for the ALI/ARDS. Therefore, we investigated whether the pendrin inhibitor showed the therapeutic effect in the LPS-induced ALI mice model.

Here, we described that a novel pendrin inhibitor (YS-01) which detected in our high-

throughput screening ameliorated LPS-induced acute lung injury in a mouse model. We also showed that the therapeutic effect of Pendrin inhibitor in ALI model come from the block both the $OSCN^-$/NF-κB-mediated inflammatory pathway.

II. MATERIALS AND METHODS

1. Experimental animals

All animal experiments were approved by the Institutional Animal Care and Use Committee of the Yonsei University College of Medicine (Seoul, Korea) and were conducted in accordance with the National Institutes of Health Guidelines for the Care and Use of Laboratory Animals. Wild-type male C57BL/6J mice, 8–10 weeks of age weighing 20– 24 g were purchased from Orient Bio (Sungnam, Republic of Korea). All animals were supplied with food and water and were subjected to a similar day and night light cycle. Transgenic nuclear factor-κB (NF-κB) reporter/ surfactant protein C (SPC)-Cre-ER^{T2} mice were used for in vivo optical imaging (IVIS) in this study. Briefly, NF-κB reporter mouse contained ROSA26 bear a lox-STOP-lox-cassette inserted between a promoter and NF-κB-luciferase-dTomato gene. Normally, the stop gene is located between loxP and loxP, and NF-κB-luciferase-dTomato were not expressed. The SPC-Cre-ER^{T2} mice were bred with ROSA26R mice to get NF-κB reporter/SPC-Cre-ER^{T2} mouse. Cre-ER^{T2} recombinase activity in these transgenic mice was induced by tamoxifen[19,20]. These NF-κB reporter/SPC-Cre-ER^{T2} mice express NF-κB activity in alveolar epithelium either dTomato fluorescence or luciferase in the presence of tamoxifen. Tamoxifen (Sigma, USA) was dissolved in a sunflower seed oil/ethanol mixture (10:1) at 10 mg/ ml. Each 4-week-old mouse was injected intraperitoneally with 100 μl of tamoxifen per day for 5 consecutive days. One week after the last injection, mice were used for IVIS or intravital imaging. Transgenic NF-κB reporter

and SPC-Cre-ER^{T2} mice were generously donated from prof. KT Nam, and prof. BC Cho working in Yonsei university.

2. Cell-based screening

CHO-K1 cells expressing human WT pendrin and YFP-F46L/H148Q/I152L were plated in 96-well microplates at a density of 2 x 10^4 cells per well and incubated for 48 h. Each well of the cell cultured in 96-well plate was washed two times with 200 μL of PBS, and it was filled with 50 μL of HEPES bufferd solution. Test compounds were added at 50 μM final concentration. After 10 minutes incubation at 37°C, the 96-well plate was placed to FLUOstar Omega microplate reader (BMG Labtech, Ortenberg, Germany) for fluorescence assay. Each well was assayed individually for pendrin-mediated I^- influx by recording fluorescence continuously (400 ms per point) for 1 s (baseline), and then 50 μL of NaI-substitued HEPES buffered solution (NaI replacing NaCl) was added using a liquid injector at 1 s and then YFP fluorescence was recorded for 5 s. Initial iodide influx rate was determined from the initial slope of fluorescence decrease, by nonlinear regression, following infusion of iodide.

3. Measurement of anion exchange

For $Cl^-/HCO3^-$ and Cl^-/OH^- measurement, intracellular pH (pHi) was measured in WT pendrin expressing CHO-K1 and MLE12 cells using pH sensor SNARF5-AM (Molecular Probes). The cells were loaded with 5 μM SNARF5-AM for 30 minutes, and then mounted in a perfusion chamber on the stage of an inverted fluorescence microscope (Nikon) equipped with a cooled charge-coupled device camera (Zyla sCMOS), an image acquisition and analysis software (Meta Imaging Series 7.7). To measure the $Cl^-/HCO3^-$ exchange activity, the $HCO3^-$ buffered solution was changed to Cl^- free $HCO3^-$ buffered solution contained (in mM): 120 Nagluconate, 5 K-gluconate,

1 MgCl2, 1 CaCl2, 10 D-glucose, 5 HEPES, and 25 NaHCO3 (pH 7.4). Applying external Cl^-free $HCO3^-$ buffered solution increases efflux of Cl^- and influx of $HCO3^-$ through pendrin. To maintain pH of $HCO3^-$ buffered solutions, the solutions were continuously gassed with 95% O2 and 5% CO2. For Cl^-/OH^- exchange measurement, HEPES buffered solution was changed to Cl^- free HEPES buffered solution for the generation of Cl gradient driving cytosolic Cl^- efflux and OH^- influx through pendrin. The SNARF5 fluorescence was recorded at excitation wavelength of 515 ± 10 nm and emission wavelength of 640 ± 10 nm, and intracellular pH calibration was performed with solutions containing 145 mM KCl, 10 mM HEPES, and 5 μM nigericin with the pH adjusted to 6.2–7.6. For Cl^-/I^- and Cl^-/SCN^- measurement, YFP fluorescence measured in pendrin and a halide sensor YFP expressing CHO-K1 cells. Cl^-/I^- exchange activity was measured as described above in cell-based screening. To measure Cl^-/SCN^- exchange activity, HEPES buffered solution was changed to NaSCN-substitued HEPES buffered solution (NaSCN replacing NaCl) for the generation of SCN^- gradient driving SCN^- influx through pendrin. YFP fluorescence changes by SCN^- influx were monitored using FLUOstar Omega microplate reader (BMG Labtech) and MARS Data Analysis Software (BMG Labtech).

4. LPS-induced acute lung injury model in mice

LPS (*Escherichia coli*, O111: B4, Sigma) (10 μg/g) in 50 μl PBS was administered by intranasal (i.n.) inhalation. Mice were lightly anesthetized by isoflurane inhalation (Abbott Laboratory) and were held in a supine position with the head elevated. The administration solution was gradually released into the nostril with the help of a microsyringe from Hamilton Com. The control group was given 50 μl of sterile PBS intranasally. For pre-treatment model, YS-01 (10mg/kg) in 50 μl DMSO was administered intra-peritoneally (i.p) 1h before LPS inhalation. For post-treatment model, two doses of YS-01 (at 6 and 12 h after LPS inhalation) was administered. The

control group was given 50 μl DMSO after PBS inhalation. The mice were sacrificed and lungs were harvested 48 h after LPS in pre-treatment group, 24h after LPS in post-treatment group. For SCN^- experiment, mice were divided into six groups, control group (DMSO+PBS+PBS), LPS group (DMSO+LPS+PBS), YS-01 group (YS01+LPS+PBS), YS-01+LPS+NaOH group, YS-01+LPS+$NaHCO_3$ group, and YS-01+LPS+NaSCN group. YS-01 (10mg/kg) in 50 μl DMSO administered intraperitoneally 1 h prior to LPS inhalation. 50 μl of NaOH, NaHCO3, NaSCN (100 mM) were administered intranasally after YS-01 treatment. PBS were administered in the same way for control, LPS, and YS-01 group.

5. Isolation of bronchoalveolar lavage

All mice were humanely killed by lethal overdose of ketamine and xylazine. Bronchoalveolar lavage fluid (BAL) was performed through a tracheal cannula using 1 ml of sterile saline. The BAL fluid (BALF) was centrifuged (4 ◦C, 3000 rpm, 10 min) and the supernatant was stored at 80◦C for further analysis. The cell pellet was reconstituted in 100 μl PBS and used for cell counts and cytospins. Total cell numbers in each sample were determined using a hemocytometer (Marienfield) according to the manufacturer's protocol. A 90 μl aliquot of each sample was transferred into the slide chambers, which were then inserted into a cytospin with the slide facing outward. The slides were centrifuged at 800 rpm for 5 min, then removed from the cytocentrifuge and dried prior to staining. Cytospins were prepared with a cytocentrifuge (Shandon Cytospin 4 cytocentrifuge, Thermo Scientific, Waltham, MA) and were stained with Diff-Quik Stain Set (Dade Behring, Newark, DE) to assess inflammation. The protein concentrations of the BAL supernatant were determined using BCA assay (Thermo Fischer Scientific). Two microliters of each sample and 198 μl of working reagent were pipetted into a microplate well and mixed thoroughly on a plate shaker for 30 s. After incubation for 30 min at 37◦C, the plate was cooled and the absorbance read at 562 nm

in a spectrophotometer.

6. Lung tissue harvest and histologic examination

The right lung was isolated and stored at −80◦C prior to protein extraction, after flushing the pulmonary vasculature with saline under low pressure. The left lung was inflated via the tracheotomy with low-melting point agarose (4%) in PBS at 25 cm H_2O pressure and until the pleural margins became sharp. The lungs were then excised and fixed overnight in 10% formaldehyde in PBS and embedded in paraffin for sectioning at 5 μm thickness. Left lung sections were stained with H&E and subjectively evaluated by light microscopy. The histopathology was reviewed in a blinded manner by two qualified investigators (EH Lee & MS Park). Five easily identifiable pathologic processes were scored using the weighted scale presented in the official ATS workshop report[21]. Lung sections were processed for immunohistochemistry using anti-rabbit SLC26A4 (ab98091, abcam) antibody.

7. ELISA

Macrophage inflammatory protein (MIP-2), interleukin-1β (IL-1ß), interleukin 6 (IL-6), and tumour necrosis factor α (TNF-α) levels in the lung lysates were measured using ELISA kits (Millipore) according to the manufacturer's directions.

8. Western blotting

Lung tissues were harvested and lysed in homogenization buffer (PRO-PREP™ Extraction solution, iNtRON BIOTECHNOLOGY). The samples were centrifuged at 13000 g for 30 min at 4 ◦C. The protein concentrations of the supernatants were

determined by using BCA assay (Thermo Fischer Scientific). Equal amounts of protein were separated by SDS/PAGE and transferred to a nitrocellulose membrane. Membranes were blocked with 5% skim milk in TBS-T (TBS (170-6435, Bio-Rad Laboratories) and 1% Tween- -20 (170-6531, Bio-Rad Laboratories) for 1h at room temperature. And then, membranes were incubated overnight with primary antibody diluted in 5% skim milk in TBS-T at 4 ℃. After washing with TBS-T, the blots were incubated with horseradish peroxidase-conjugated secondary antibodies and 5% skim milk in TBS-T for 1 h at room temperature and developed using Super-Signal West Pico chemiluminescence detection kit (Pierce). The antibodies used in the present study included rabbit SLC26A4 (ab98091, abcam), mouse phospho-IκB (9246, Cell Signaling Technology), mouse IκB (4814, Cell Signaling Technology), rabbit α-tubulin (PA5-16891, Cell Signaling Technology). Quantification of Western blots was conducted by ImageJ (Image Processing and Analysis in Java, NIH, USA) software.

9. In vivo optical imaging (IVIS)

Imaging of live animals or organs was performed using an IVIS Kinetic imaging system (Caliper Life Sciences, Preston Brook Runcorn, UK). The IVIS system consisted of a cooled charge-coupled device (CCD) camera mounted onto a light-tight specimen chamber. The fluorescent excitation light was provided by a halogen lamp in combination with appropriate excitation filters. Emission filters were placed in front of the camera aperture to allow recording of specific wavelengths of light, depending on the emission spectra of the FP examined. Fluorescence imaging was obtained with an excitation wavelength of 554 nm and emission wavelength of 581 nm (dTomato). NF-κB reporter/SPC-Cre-ER^{T2} Mice were divided three groups for IVIS imaging, i) DMSO + PBS, ii) DMSO+LPS, iii) YS-01 (10mg/kg, i.p) + LPS and *ex vivo* lungs were aseptically removed 6 hours after LPS treatment. When organs were imaged, they were placed as flatly as possible to allow full and consistent light penetration in order to

minimize potential variation in the measurements due to different tissue thickness. Fluorescence was quantified by using the Region of Interest (ROI) tool in the Living Image software (version 3.2, Caliper Life Sciences).

10. Human bronchoalveolar lavage fluid collection

This study combined the results from two prospective study. 48 patients suspected pulmonary infection who underwent a bronchoalveolar lavage (BAL) classified pneumonia group. And the 25 patients who were admitted for evaluation of lung masses without evidence of pulmonary infection were classified as the control group at the Severance Hospital between May 2013 and September 2015.

Prior to bronchoscopy, subjects received a topical anaesthesia (lidocaine) by nebulizer and then were sedated with midazolam and fentanyl. The bronchoscope was inserted and wedged into the mouth for the BAL. BAL was performed following a standardized protocol (Infection: bronchus of pulmonary lesion, Control: opposite bronchus from lung mass) and 10 cc of BALF was acquired from each patient using about 30 ml sterile 0.9% saline. BALF was centrifuged (10 min; 1500 g) and the supernatant was cryopreserved at −80 ◦C until use.

A total of 73 patients were included in this study; 25 patients were classified as control group and 48 patients with pulmonary infection as infection group. Demographic and clinical data, including age, gender, body mass index (BMI), comorbidities, BALF analysis, cause of pneumonia and final diagnosis were obtained from each participant and medical record. The pendrin levels of supernatant were measured using human SLC26A4 ELISA kit (MBS764789, Mybiosource) according to the manufacturer's directions.

11. Ethics statement

All animal protocols were approved by the Institutional Animal Care Committee of the Medical College of Yonsei University (2016-0322). All animal experiments were conducted in accordance with the recommendations in the Guide for the Care and Use of Laboratory Animals of the National Institutes of Health.

Human study protocols were reviewed and approved by the Institutional Review Board of Yonsei University Health Service, Severance Hospital, Seoul, Korea (Pneumonia group IRB No. 4-2013-0585, Control group IRB No. 4-2014-1014). Informed consent was obtained from patients or their guardians about the use of the BALF samples.

12. Statistical Analysis

Statistical analysis was performed using Prism 5.0 (GraphPad Software). Group comparisons were performed using 2-tailed Student's t test to compare 2 groups, 1-way ANOVA to compare more than 2 groups. Data are expressed as means ± SEM. $P < 0.05$ was considered statistically significant. All in vivo and in vitro experiments were repeated a minimum of 3 independent times.

III. RESULTS

1. Absence of LPS-induced acute lung injury in pendrin-null mice

To investigate the role of pendrin in LPS induced acute lung injury (ALI), we first compared the effect of LPS treatment (instillation) in wild-type (WT) mice and in pendrin knock out (KO) mice (n=6-8 mice/group). As expected, the number of total cell count in bronchoalveolar lavage fluid (BALF) was markedly increased in WT mice after LPS, compared to PBS treatment (vehicle control) (Figure 1A). And the protein

concentration of BAL fluid, reflecting vascular permeability, were also increased in WT mice after LPS (Figure 1B). In contrast, pendrin KO mice displayed much reduced levels of total cell count and protein concentration in BALF, relative to WT mice (Figure 1A and 1B). In addition, assessment of lung pathology revealed a significant decrease in leukocytes infiltration and lung injury in pendrin KO mice, relative to pendrin WT mice after LPS treatment (Figure 1C). These results suggested that pendrin has important roles in the development of LPS induced ALI.

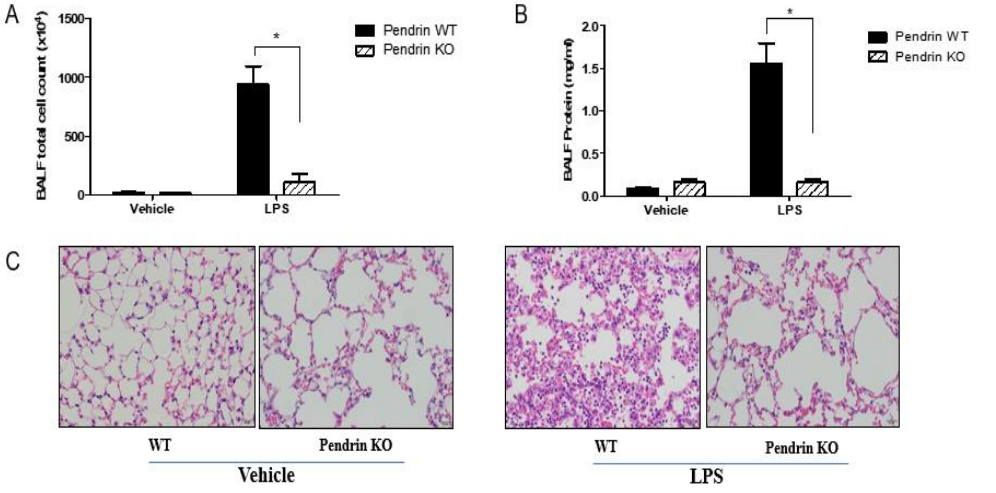

Figure 1. Deficiency of pendrin attenuated LPS induced lung injury in pendrin KO mice. Pendrin wide-type (WT) or knock-out (KO) mice were instilled LPS (10 μg/g) intranasally (i.n.) or vehicle (PBS). (A) Total bronchoalveolar lavage (BAL) cell counts, (B) BAL protein concentration, analyzed 48hrs after LPS or PBS instillation, (C) Representative images of H&E stain of lung tissue 48hrs after LPS or PBS instillation (x400), Data are means ± SEM (n = 6-8 mice per group), *<0.05, **P < 0.01, analyzed by 1-way ANOVA with post hoc test. LPS=lipopolysaccharide; PBS= phosphate-buffered saline; H&E = hematoxylin and eosin.

2. Screening of pendrin inhibition and its effect in alveolar epithelia

We next performed a cell-based high-throughput screening for the identification of potent and selective pendrin inhibitors. In Brief, Screening of 54,400 diverse compounds and structure-activity studies revealed a novel pendrin inhibitor, YS-01. We

first observed the effects of YS-01 on Cl^-/anion exchange activities. Cl^-/I^- and Cl^-/SCN^- exchange activity were measured using YFP quenching assay in CHO-K1 cells expressing pendrin and YFP-F46L/H148Q/I152L (Figure 2), Cl^-/HCO_3^- and Cl^-/OH^- exchange activity were monitored using intracellular pH sensor SNARF5 in CHO-K1 cells expressing pendrin. YS-01 potently inhibited all modes of pendrin-mediated Cl^-/I^-, Cl^-/SCN^-, Cl^-/HCO_3^- and Cl^-/OH^- exchange activity.

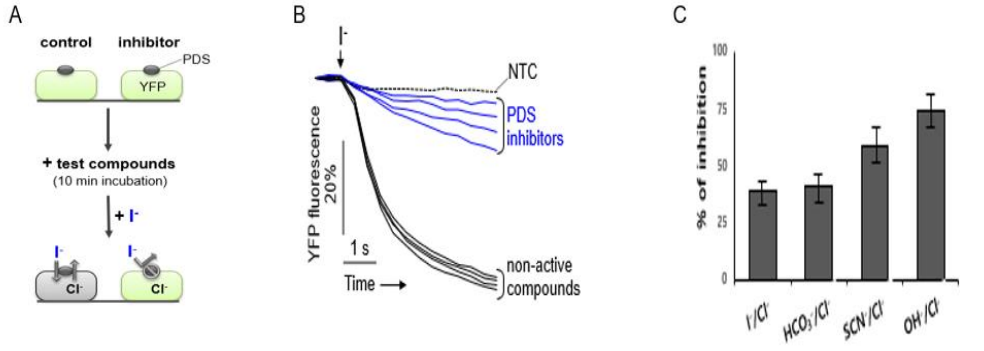

Figure 2. Screening of small molecule for pendrin inhibition. Pendrin inhibitor (YS-01) potently inhibited all modes of pendrin-mediated Cl^-/I^-, Cl^-/SCN^-, Cl^-/HCO_3^- and Cl^-/OH^- exchange activity.

3. Pendrin inhibitor attenuated the phenotype of LPS-induced acute lung injury in mice.

To investigate the protective function of YS-01 in LPS induced ALI mice model, we treated YS-01 one hour before LPS intranasal instillation and mice were sacrificed 48 hours after LPS administration (Figure 3A-1). Total cell count and protein concentration of BALF were markedly increased in LPS-treated group compared to vehicle treated group. In contrast, YS-01(10mg/kg) pre-treated mice displayed reduced levels of total cell count and protein concentration in BALF, relative to vehicle treated mice (Figure 3A-2 and A-3). The BALF protein level gradually decreased after

intraperitoneal injection of YS-01 in a dose dependent manner (Figure 3A-4). YS-01 pre-treatment also significantly reduced the lung injury score, compared with vehicle treated mice where the infiltration of leukocytes after LPS exposure was suppressed (Figure A-5 and A-6).

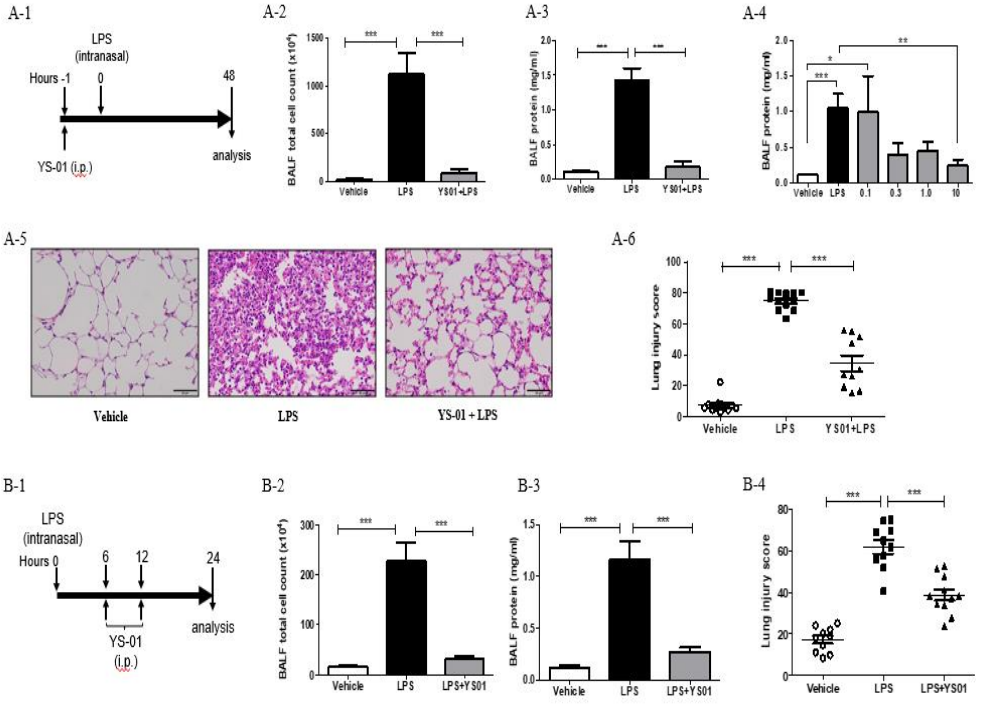

Figure 3. Pendrin inhibitor (YS-01) suppress the phenotype of LPS-induced acute lung injury in mice. C57BL/6J mice were instilled LPS (10 mg/kg) intranasally. (A-1) YS-01 (10mg/kg) was intraperitoneally injected 1h before LPS (Pre-treatment) or (B-1) 6h, 12h after LPS (post-treatment). (A-2) BALF total cell count, (A-3) BALF protein concentration, (A-4) BALF protein concentration according to various YS-01 concentrations, (A-5) Representative images of H&E stain of lung tissue 48h after LPS or PBS administration (x400) and lung injury score of YS-01 pre-treatment experiment. Infiltration of inflammatory cells and lung injury were reduced by YS-01 treatment. (B-2) BALF total cell count, (B-3) BALF protein concentration, (B-4) lung injury score of YS-01 post-treatment experiment. Data are means ± SEM (n=10-12 mice per group), ***P < 0.001, analyzed by 1-way ANOVA with post hoc test.

We also determined whether YS-01 treatment was effective after LPS injury. Two doses of YS-01 (10mg/kg at 6 and 12 h after LPS) was administered and mice were sacrificed 24 hours after LPS (Figure 3B-1). YS-01 treatment after LPS also significantly reduced total cell count and protein concentration of BALF as well as lung injury score, consistent with YS-01 pre-treatment experiment (Figure 3B-2, B-3 and B-4).

4. NaSCN instillation obscure the effect of pendrin inhibitor in ALI mice model

To address the mechanism underlying the therapeutic effect of YS-01 in LSP-induced ALI, we supplied OH^-, HCO_3^-, SCN^- which were the anions secreted by the pendrin. Intranasal application of NaSCN (50 μl of 100 mM) blocked the protective effects of YS-01 in LPS induced ALI so that total cell count, protein concentration of BALF and lung injury score were increased as the group LPS treated alone. However, administration of NaOH, $NaHCO_3$ did not change the effect of YS-01 in LPS-induced ALI mice (Figure 4A and 4B). Histological analysis also revealed that protective effect of YS-01 on infiltration of inflammatory cells and lung injury after LPS was also abolished by the administration of NaSCN (Figure 4C and 4D). These data indicate that the therapeutic effect of YS-01 comes from the inhibition of SCN^- transport function of pendrin.

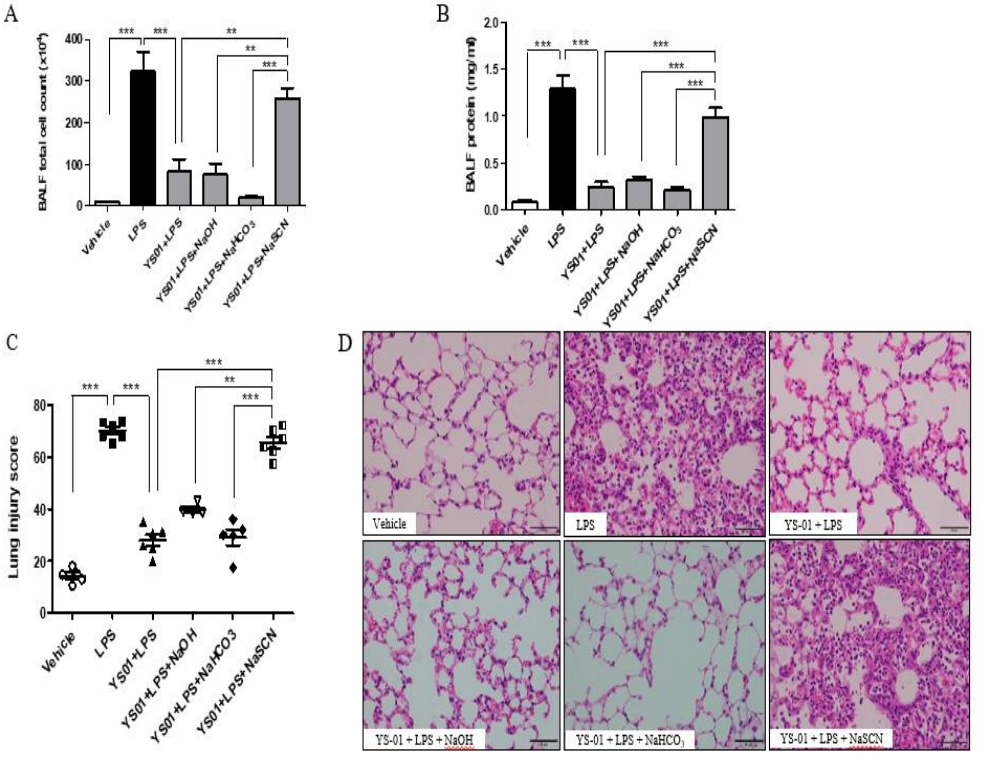

Figure 4. SCN^- blocks the protective effects of YS-01 in LPS induced mouse lung injury. Mice were instilled LPS (10 μg/g) intranasally (i.n.). The YS01 (10mg/kg, i.p) treated mice were nasally administered with 50 μl of NaOH, $NaHCO_3$, NaSCN (100 mM). (A) BALF total cell count, (B) BALF protein concentration, (C) Lung injury score, (D) Representative histology of lung tissue stained with hematoxylin and eosin (x400). Data are means ± SEM (n = 5-6 per group). *<0.05, **P < 0.01, ***P<0.001, analyzed by 1-way ANOVA with post hoc test.

5. Pendrin inhibitor suppress the NF-kB pathway and decrease inflammatory cytokine in LPS-induced ALI mice model

We further dissected the singling pathway by which the YS-01 working in LPS-induced ALI model using NF-κB reporter/SPC-Cre-ER^{T2} mice. To determine quantitative amount fluorescence, we evaluated IVIS image of mice lungs. Lungs were aseptically removed right before imaging. Fluorescence of LPS treated lungs were increased,

compare to PBS treated lungs. In the YS-01 treated group, fluorescence was lower, relative to vehicle (DMSO) treated mice (Figure 5A-1 and 5A-2). These results suggesting that NF-κB activation in LPS exposed mice were suppressed by pendrin inhibitor YS-01. Immunoblot analysis showed that NF-κB pathway is associated with pendrin inhibitor action. Phospho-IκB protein expression which represent NF-κB activation was increased after LPS (Figure 5B-1 and 5C-1), and pendrin inhibitor YS-01 treatment before LPS or after LPS both significantly reduced Phospho-IκB expression.

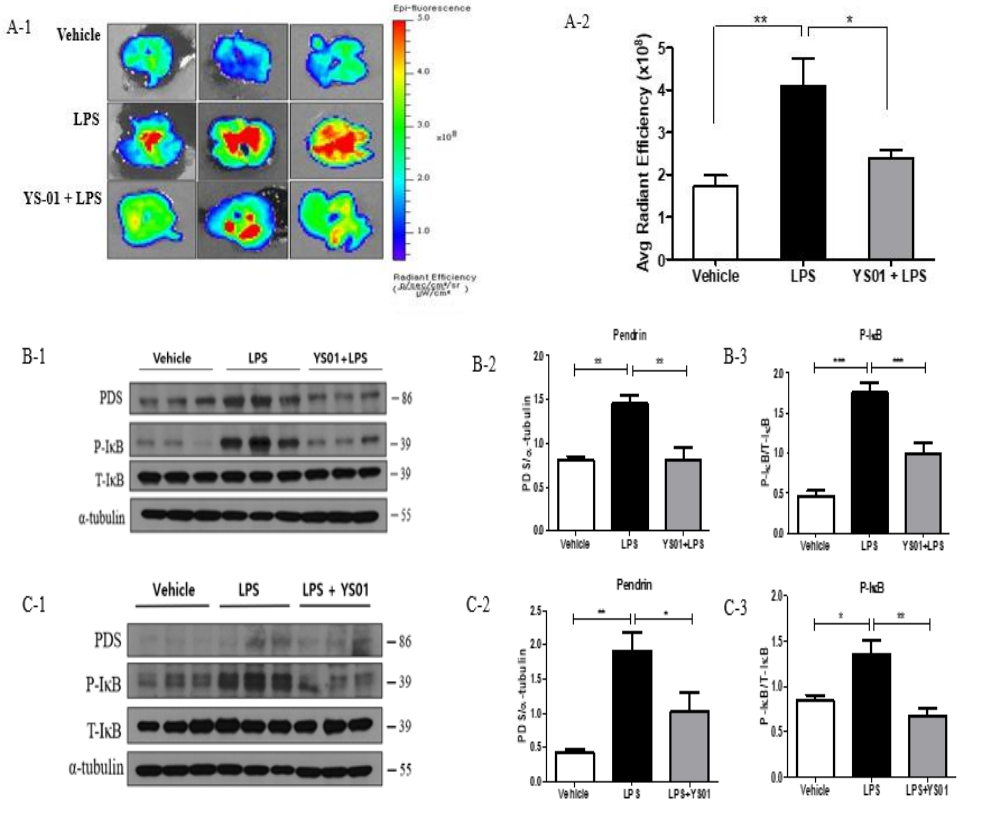

Figure 5. Pendrin inhibitor (YS-01) blocks the NF-kB pathway in LPS induced acute lung injury. Mice were killed at 6h after LPS (10 μg/g) administration and lungs were imaged via IVIS systems. YS-01 (10mg/kg) was intraperitoneally injected 1h before LPS. (A-1) *Ex vivo* imaging of lungs from NF-κB/SPC-Cre mice exposed with LPS and treated with YS-01 or

vehicle, IVIS image, fluorescence is presented as radiant efficiency, (A-2) Average fluorescence was quantified by ROI analysis using Living Image software. Data are means ± SEM (n = 9-10 mice per group). (B and C) Representative western blot analysis and relative protein levels by densitometry for pendrin and phospho-IκB in lung lysates (60 μg). Mice were instilled LPS (10 μg/g) intranasally. YS-01 (10mg/kg) was intraperitoneally injected 1h before LPS (Pre-treatment, B) or 6h, 12h after LPS (post-treatment, C). (means ± SEM, n = 6 per group), *<0.05, **P < 0.01, **P < 0.001, analyzed by 1-way ANOVA with post hoc test.

The levels of cytokines, such as IL-1ß, tumor necrosis factor-α, Macrophage inflammatory protein (MIP)-2 were significantly increased after LPS, compare with PBS (Figure 6A). IL-6 tended to be increased, relative to PBS, although statistically insignificant. In contrast, levels of pro-inflammatory cytokines were decreased in YS-01 pre-treatment mice, relative to vehicle (DMSO) treatment after LPS (Figure 6A). We also observed similar results in YS-01 post-treatment experiments although statistical significance was insufficient (Figure 6B).

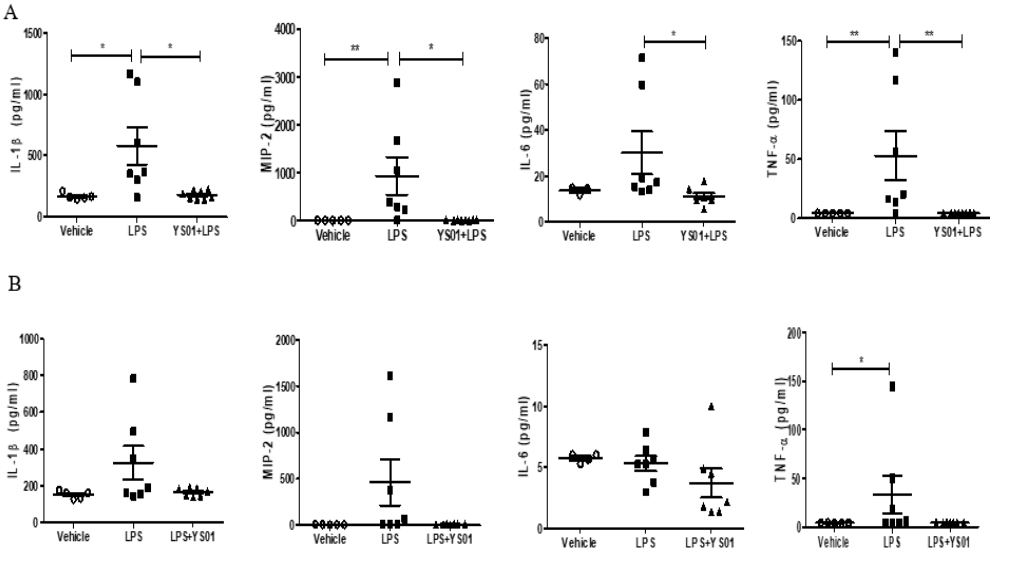

Figure 6. Inflammatory cytokines were reduced in mice with YS-01 pre or post treatment in LPS induced lung injury. IL-1β, CXCL2/MIP-2, IL-6, and TNF-α cytokine levels were measured in lung tissue lysates by ELISA (A) YS-01 Pre-treatment, (B) YS-01 post-treatment,

Data are means ± SEM (n = 7-8 mice per group). *<0.05, **P < 0.01, analyzed by 1-way ANOVA with post hoc test.

6. Pendrin levels are increased in patients with pulmonary infection

To translate our in vitro and in vivo findings to human disease, we measured pendrin protein expression in BALF of patients with pneumonia and patients with lung mass without infection (control group). The clinical characteristics of the study patients are summarized in Table 1.

We observed that pendrin levels were significantly elevated in BALF of patients with pneumonia (n=48) compared with control subjects (n=25) (mean, 22.65 vs. 6.83 ng/ml, p<0.001) (Figure 7).

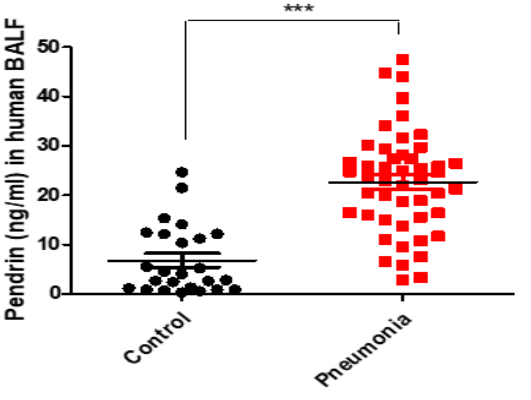

Figure 7. SLC26A4 (pendrin) levels of human BALF in patients with pulmonary infection increased compared to control patients without infection.

SLC26A4 (pendrin) levels were measured from supernatant of human BALF by ELISA (Control n = 25, Peumonia n=48). *P<0.05, **P<0.01, ***P<0.001 analyzed by student's unpaired 2-tailed t test.

Table 1. Clinical characteristics of study patients

	Control (n=25)	Pneumonia (n=48)	*P*
Age, years, mean ± SD	63.8 ± 9.7	61.9 ± 16.8	0.544
Gender, male, N (%)	20 (80.0)	36 (75.0)	0.631
BMI (kg/m2), mean ± SD	24.5 ± 4.3	22.3 ± 3.3	0.022
ICU admission, N (%)	0	41 (85.4)	
Intubation/ARDS, N (%)	0	41 (85.4)	
P/F ratio, mean ± SD	−	189.9 ± 94.3	
Bacteremia, N (%)	0	9 (18.8)	
Length of stay, d, median (IQR)	2 (1-2)	31 (19-48)	
28-day mortality, N (%)	0	20 (41.7)	
In-hospital mortality, N (%)	0	28 (58.3)	
Pendrin Level, ng/ml, mean ± SD	6.83 ± 6.91	22.65 ± 10.43	<0.001

Values are presented as the mean±SD, median (interquartile range, IQR), or number (%)

Abbreviations: BMI, body mass index; ARDS, acute respiratory distress syndromes.

IV. DISCUSSION

Emerging evidences strongly suggests that the pendrin is one of the key protein in the airway inflammatory disease such as asthma, COPD and rhinitis[13,22]. Recent report also showed that pendrin expression was enhanced in lipopolysaccharide-induced acute lung injury murine model, and non-specific pendrin inhibitor attenuated acute lung injury in mice[18]. In this study, we showed that the expression of pendrin in BALF of the patients with pneumonia and LPS-treated mouse was increased. Moreover, we demonstrated that LPS-induced ALI did not induced in pendrin null mice, which strongly indicate the critical role of pendrin in the pathogenesis of ALI. These evidences encourage us to development of Pendrin inhibitors as a novel drug for the ALI/ARDS.

We screened a specific pendrin inhibitor (YS-01) which did not affect other ion transport such as CFTR and CaCC. YS-01 almost completely prevented the development of LPS-induced acute lung injury in mice. Furthermore, administration of YS-01 after LPS treatment also attenuated the lung injury caused by LPS in mice. These findings suggest the utility of pendrin inhibitors in the treatment of acute lung injury.

The role of pendrin and the mechanism of pendrin inhibitor underlying the preventive or therapeutic effects in the ALI model is unclear. We focused on the Cl^-/SCN^- exchange activity of pendrin and $OSCN^-$ which can be crucial role in the airway inflammation. Hypothiocyanite ($OSCN^-$) is known to act as an important innate defense system against microbes in the airways[23,24], which is generated by the catalysis of peroxidases using SCN^- transported via several anion transporters including Pendrin. Recent studies showed that increased hypothiocyanite ($OSCN^-$) production by upregulation of pendrin induced the airway inflammation in allergic asthma model via activation of NF-κB cascade [25,26].

We showed that YS-01 inhibited the LPS-induced NF-κB activation and subsequent cytokine production in murine ALI model. Furthermore, the preventive effect of YS-01 on ALI disappeared when we add the NaSCN into the airway of mice. There data collectively indicated the mode of action of pendrin inhibitor. YS-01 block the transepithelial transport of SCN^- and subsequently inhibited $OSCN^-$ generation and NF-κB activation, which result in suppression of proinflammatory cytokines (Figure. 8). This is a very similar mode of action in our another ongoing study where pendrin inhibitors attenuated OVA-induce allergic airway inflammation by inhibition of pendrin/$OSCN^-$/Nf-κB cascade. Previous report also showed that high dose of $OSCN^-$ can induce airway epithelial cell death so that pendrin inhibitor could prevent cell death by reducing $OSCN^-$ production [25,26].

Although the critical care for the patients with ALI have been improved, the mortality of ALI/ARDS is still high and there are limited options for the medical treatment of

ALI/ARDS. Because the pendrin inhibitor, YS-01 showed strong therapeutic effect on ALI murine model, pendrin can be a novel target for the medical treatment of ALI/ARDS. However, there are still several issues to be solved for the clinical application of pendrin as a drug in ALI/ARDS treatment. Even though the most patients who carry homozygote pendrin mutation only shows prelingual hearing loss without any phenotype, the systemic adverse effect of pendrin inhibitors must be ruled out where the pendrin is expressed including inner ear, thyroid, and kidney. We can avoid these potential side effects by local administration of pendrin inhibitors in patients with ALI. Another important issue for the development of pendrin inhibitors as a drug is specificity of YS-01 on pendrin. Especially, our data in another report showed that YS-01 weakly stimulate SLC26A3 (DRA) and SLC26A6 so that it can exert biological effect in intestine and kidney. Nevertheless, YS-01 is chemically stable with low cytotoxicy and works in nanomolar level so we think YS-01 can be a tool compound for the further development of candidate for the clinical trials. One promising data is that the expressions of pendrin were upregulated in BALF of pneumonia patients so pendrin inhibitors can works effectively in these patients. Further large-scale study is needed to determine whether pendrin expression is associated with disease severity or prognosis of ALI/ARDS patients.

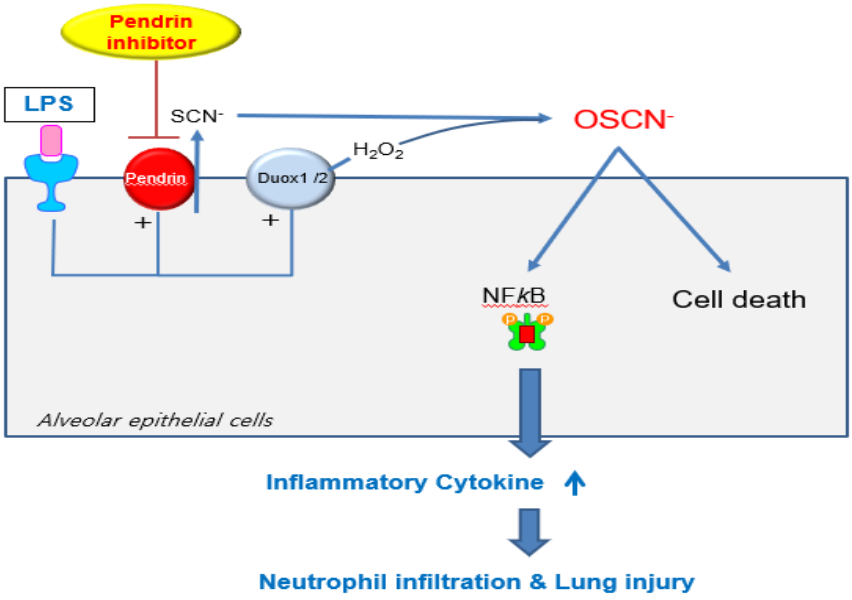

Figure 8. Schematic diagram of the action of pendrin inhibitor which suppress the $OSCN^-$ production and its activation of NF-κB in alveolar epithelial cells. SCN^- is actively transported into pulmonary lumens via pendrin/SLC26A4 at the apical side in alveolar epithelial cells. SCN^- together with H_2O_2 generated by Duox1 and Duox2 is catalyzed by peroxidases into $OSCN^-$. The produced $OSCN^-$ activates NF-κB and cause inflammatory cytokine release and neutrophil infiltration and subsequent lung injury. Pendrin inhibitor (YS-01) blocks the transepithelial transport of SCN^- which inhibited $OSCN^-$ generation and NF-κB activation subsequent event of ALI.

V. CONCLUSION

In summary, our data suggested that the possible clinical benefit of Pendrin inhibitors in the treatment of patients with ALI. In particular, our data showed that post-treatment of Pendrin inhibitor after LPS application also showed therapeutic effect in mice model. These data indicate clinical therapeutic window for Pendrin inhibitors is wide including post-ALI periods. In conclusion, a small molecule which inhibits pendrin potently attenuated LPS induced ALI in mice. Thus, this study provides insight that pendrin inhibitor may be a promising new class of candidate for treatment of ALI/ARDS.

REFERENCES

1. Goss CH, Brower RG, Hudson LD, Rubenfeld GD. Incidence of acute lung injury in the United States. Crit Care Med 2003;31:1607-11.
2. Zambon M, Vincent JL. Mortality rates for patients with acute lung injury/ARDS have decreased over time. Chest 2008;133:1120-7.
3. Erickson SE, Martin GS, Davis JL, Matthay MA, Eisner MD. Recent trends in acute lung injury mortality: 1996-2005. Crit Care Med 2009;37:1574-9.
4. Fan E, Needham DM, Stewart TE. Ventilatory management of acute lung injury and acute respiratory distress syndrome. Jama 2005;294:2889-96.
5. Wheeler AP, Bernard GR. Acute lung injury and the acute respiratory distress syndrome: a clinical review. Lancet 2007;369:1553-64.
6. Mutlu GM, Sznajder JI. Mechanisms of pulmonary edema clearance. Am J Physiol Lung Cell Mol Physiol 2005;289:L685-95.
7. Scott DA, Wang R, Kreman TM, Sheffield VC, Karniski LP. The Pendred syndrome gene encodes a chloride-iodide transport protein. Nat Genet 1999;21:440-3.
8. Soleimani M, Greeley T, Petrovic S, Wang Z, Amlal H, Kopp P, et al. Pendrin: an apical Cl-/OH-/HCO3- exchanger in the kidney cortex. Am J Physiol Renal Physiol 2001;280:F356-64.
9. Pedemonte N, Caci E, Sondo E, Caputo A, Rhoden K, Pfeffer U, et al. Thiocyanate transport in resting and IL-4-stimulated human bronchial epithelial cells: role of pendrin and anion channels. J Immunol 2007;178:5144-53.
10. Sala-Rabanal M, Yurtsever Z, Berry KN, Brett TJ. Novel Roles for Chloride Channels, Exchangers, and Regulators in Chronic Inflammatory Airway Diseases. Mediators Inflamm 2015;2015:497387.
11. Everett LA, Glaser B, Beck JC, Idol JR, Buchs A, Heyman M, et al. Pendred

syndrome is caused by mutations in a putative sulphate transporter gene (PDS). Nat Genet 1997;17:411-22.

12. Everett LA, Belyantseva IA, Noben-Trauth K, Cantos R, Chen A, Thakkar SI, et al. Targeted disruption of mouse Pds provides insight about the inner-ear defects encountered in Pendred syndrome. Hum Mol Genet 2001;10:153-61.
13. Nakao I, Kanaji S, Ohta S, Matsushita H, Arima K, Yuyama N, et al. Identification of pendrin as a common mediator for mucus production in bronchial asthma and chronic obstructive pulmonary disease. J Immunol 2008;180:6262-9.
14. Ishida A, Ohta N, Suzuki Y, Kakehata S, Okubo K, Ikeda H, et al. Expression of pendrin and periostin in allergic rhinitis and chronic rhinosinusitis. Allergol Int 2012;61:589-95.
15. Adams KM, Abraham V, Spielman D, Kolls JK, Rubenstein RC, Conner GE, et al. IL-17A induces Pendrin expression and chloride-bicarbonate exchange in human bronchial epithelial cells. PLoS One 2014;9:e103263.
16. Scanlon KM, Gau Y, Zhu J, Skerry C, Wall SM, Soleimani M, et al. Epithelial anion transporter pendrin contributes to inflammatory lung pathology in mouse models of Bordetella pertussis infection. Infect Immun 2014;82:4212-21.
17. Haggie PM, Phuan PW, Tan JA, Zlock L, Finkbeiner WE, Verkman AS. Inhibitors of pendrin anion exchange identified in a small molecule screen increase airway surface liquid volume in cystic fibrosis. Faseb j 2016;30:2187-97.
18. Jia CE, Jiang D, Dai H, Xiao F, Wang C. Pendrin, an anion exchanger on lung epithelial cells, could be a novel target for lipopolysaccharide-induced acute lung injury mice. Am J Transl Res 2016;8:981-92.
19. el Marjou F, Janssen KP, Chang BH, Li M, Hindie V, Chan L, et al. Tissue-specific and inducible Cre-mediated recombination in the gut epithelium. Genesis 2004;39:186-93.

20. Gui YS, Wang L, Tian X, Feng R, Ma A, Cai B, et al. SPC-Cre-ERT2 transgenic mouse for temporal gene deletion in alveolar epithelial cells. PLoS One 2012;7:e46076.
21. Matute-Bello G, Downey G, Moore BB, Groshong SD, Matthay MA, Slutsky AS, et al. An official American Thoracic Society workshop report: features and measurements of experimental acute lung injury in animals. Am J Respir Cell Mol Biol 2011;44:725-38.
22. Yick CY, Zwinderman AH, Kunst PW, Grunberg K, Mauad T, Dijkhuis A, et al. Transcriptome sequencing (RNA-Seq) of human endobronchial biopsies: asthma versus controls. Eur Respir J 2013;42:662-70.
23. Chandler JD, Min E, Huang J, Nichols DP, Day BJ. Nebulized thiocyanate improves lung infection outcomes in mice. Br J Pharmacol 2013;169:1166-77.
24. Chandler JD, Min E, Huang J, McElroy CS, Dickerhof N, Mocatta T, et al. Antiinflammatory and Antimicrobial Effects of Thiocyanate in a Cystic Fibrosis Mouse Model. Am J Respir Cell Mol Biol 2015;53:193-205.
25. Suzuki S, Ogawa M, Ohta S, Nunomura S, Nanri Y, Shiraishi H, et al. Induction of Airway Allergic Inflammation by Hypothiocyanite via Epithelial Cells. J Biol Chem 2016;291:27219-27.
26. Izuhara K, Suzuki S, Ogawa M, Nunomura S, Nanri Y, Mitamura Y, et al. The Significance of Hypothiocyanite Production via the Pendrin/DUOX/Peroxidase Pathway in the Pathogenesis of Asthma. Oxid Med Cell Longev 2017;2017:1054801.

ABSTRACT (IN KOREAN)

Lipopolysaccharide 유도 급성 폐손상 동물모델에서 약물 스크리닝을 통해 새롭게 발굴된 펜드린 억제제의 효과

<지도교수 박 무 석>

연세대학교 대학원 의학과

이 은 혜

목적: 펜드린(pendrin)은 SLC26A4 에 의해 암호화(encode)되는 음이온교환제로, 최근 여러 연구에서 COPD, 알레르기 비염, 천식과 같은 기도 질환에서 펜드린의 발현이 증가되어 있음을 보고하였다. 하지만 염증 매개 급성 폐손상에서 펜드린의 역할에 대한 연구는 부족한 실정이다. 본 연구에서는 lipopolysaccharide(LPS) 유도 급성 폐손상 (acute lung injury) 동물 모델에서 펜드린의 발현과, 새로운 펜드린 억제제 (YS-01)의 역할을 규명하고자 하였다.

방법: 마우스 비강내로 LPS(10 μg/g)를 주입하고 DMSO 또는 펜드린 억제제(YS-01)를 복강주사로 투여하였다. 폐손상 정도는 폐 조직 및 기관지폐포세척액(bronchoalveolar lavage fluid, BALF)에서 평가하고 염증성 사이토카인을 폐 조직에서 측정하였다. 생체내 광학 이미징(IVIS) 측정을 위해 NF-κB reporter/SPC-Cre-ER^{T2} 마우스를 사용하였다. 또한

48 명의 폐렴 환자와 25 명의 비감염성 질환 환자의 기관지폐포세척액에서 펜드린 수치를 측정하였다.

결과: YS-01 과 LPS 를 투여한 마우스는 DMSO 와 LPS 를 투여한 마우스에 비해 폐손상이 감소되었고, 기관지폐포세척액에서 염증세포 수 및 단백질 농도가 감소하였다. 염증성 사이토카인은 LPS 투여시 증가하였으며, YS-01 치료 후에 다시 억제되었다. Western blot 과 생체내 광학 이미징(IVIS)로 분석한 NF-κB 활성화는 LPS 를 주입한 마우스에서 YS-01 처리시 억제되는 결과를 보였다. 또한 폐렴 환자의 기관지폐포세척액에서 측정한 펜드린의 수치는 비감염성질환 환자의 기관지폐포세척액보다 그 농도가 통계적으로 유의하게 낮았다 (평균값, 22.65 vs. 6.83 ng/ml, $p<0.001$).

결론: 본 연구의 결과는 펜드린 억제제가 향후 패혈증 매개 급성 폐손상을 포함한 염증성 기도 질환의 치료에 새로운 치료 전략이 될 수 있음을 시사한다.

핵심되는 말: 펜드린, 억제제, SLC26A4, 급성 폐손상